

Measurement of Hydroxyl Concentrations in Air Using a Tunable uv Laser Beam

Charles C. Wang and L. I. Davis, Jr.

Scientific Research Staff, Ford Motor Company, Dearborn, Michigan 48121

(Received 8 November 1973)

We report the first measurement of hydroxyl (OH) concentrations in air by detecting the resonance fluorescence excited by tunable radiation near 2825.8 Å. On a particular day, the OH concentrations deduced from these measurements ranged from a high of 1.5×10^8 OH/cm³ in the early afternoon to a level below 5×10^6 OH/cm³ at night.

This Letter reports the first measurement of hydroxyl (OH) concentrations in air by detecting the resonance fluorescence excited by a tunable laser source in the ultraviolet.¹ Weinstock² has pointed out that OH plays a central role in smog formation and in controlling the global concentrations of carbon monoxide and methane. The ability to measure ambient concentrations of OH should afford an accurate determination of numerous photochemical cycles operative in either polluted or natural atmosphere. However, the ambient concentration of OH has never been established experimentally, and various estimates^{2,3} yield results ranging from 7×10^4 to 5×10^8 OH/cm³.

In performing the experiments in the laboratory, it was observed that the OH concentration in air varied during the course of the day. On a particular day, it ranged from a value of 1.5×10^8 OH/cm³ in the early afternoon (~2:00 p.m.), to 1.6×10^7 OH/cm³ at around 6:00 p.m., and to a level below our present detection limit of 5×10^6 OH/cm³ (0.2 part per 10^{12} in air) at night (~10:30 p.m.). The OH concentration also dropped to a level below the detection limit when it was raining or overcast outside, or when the ventilation system was shut off to prevent the fresh air outside from getting into the laboratory. It was estimated that a significant portion of the air near the focal region came from outside the laboratory with a transport time of about 6 sec. We are currently improving the collection efficiency of our optics by a factor of 10, and expect to monitor the diurnal variation of OH concentration in air both inside the laboratory and outside.

The experiments were performed with a tunable source near the $P_1(2)$ line (2825.8 Å) in the ${}^2\Pi(v=0) \rightarrow {}^2\Sigma^+(v=1)$ transitions⁴ of OH. The light source near 2825.8 Å was derived from the second harmonic of the output from a dye laser system; the latter consisted of one oscillator and two amplifier stages,⁵ and were operated with rhodamine S dissolved in methanol and at a rep-

etition rate of one pulse every 10 sec. Frequency narrowing was accomplished using a Littrow grating as an end reflector and an intracavity Fabry-Perot etalon. Fine tuning was done by varying the mixture of helium and propylene which filled the etalon spacing. The output pulse from the laser typically measured 50 mJ in energy and 0.4 cm^{-1} in spectral width, and lasted about 0.5 μsec. The second harmonic of the output was generated in a 5-cm crystal of ammonium dihydrogen phosphate oriented for index matching. With optimal focusing, an output energy of up to 6 mJ per pulse at the second harmonic frequency was obtained.

Figure 1 depicts a schematic of the experimental setup. The second harmonic beam near 2825.8 Å was focused in air to a spot 2 mm in diameter, and the scattered light emanating in a direction 90° from the exciting radiation was collected with $f/3.5$ optics, processed through two Spex Model 1700 spectrometers operated in tandem, and detected by a high-gain photomultiplier and related photon counting apparatus. Extensive experiments⁶ performed with a tightly focused beam indicate that careful consideration be taken to avoid the interference due to two-photon dissociation of water, which generates OH. A large focal spot was used so as to reduce this interference to a negligible level. The background count due to the dark current of the photon counting apparatus

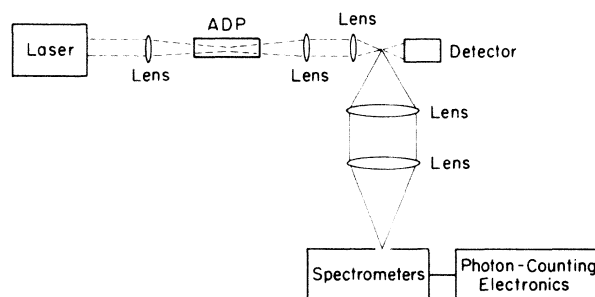


FIG. 1. Schematic of the experimental setup.

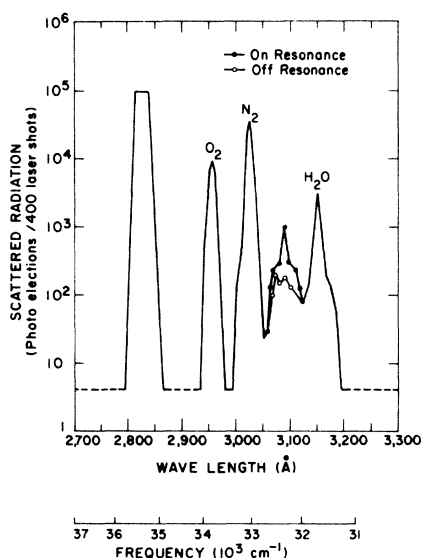


FIG. 2. Spectrum of the scattered light excited in air by the incident radiation near 2825.8 Å. The peaks at 2956, 3025, and 3151 Å are due, respectively, to the spontaneous Raman scattering of oxygen, nitrogen, and water in air. The gratings used were 1200 lines/mm and blazed at 3000 Å. The combined resolution of the spectrometers was 15 Å.

was measured to be less than one photoelectron per 1000 laser shots; and the background count due to internal scattering inside the spectrometers was measured to be less than one event per 100 laser shots in the region of OH fluorescence.

The spectrum of the scattered light excited by the second harmonic beam near 2825.8 Å in air is shown in Fig. 2. Aside from the familiar features due to the spontaneous Raman scattering in air, the band centered near the 3090 Å is of particular interest. It was observed that the intensity of this band depended very sensitively on the exact frequency of the exciting radiation (Fig. 3), whereas the other features in Fig. 2 did not. It follows from this resonant nature of the excitation process that the signal near 3090 Å is due to resonance fluorescence or resonant Raman scattering excited by the incident radiation. From a consideration of the collisional relaxation of OH in the excited state⁶ and the experimental results obtained at high OH concentrations,² it is anticipated that excitation of OH by absorbing the radiation near 2825.8 Å would result in fluorescence centered around 3090 Å due to the ${}^2\Sigma^+(v=0) \rightarrow {}^2\Pi(v=0)$ transitions of OH. To ascertain that the observed signal near 3090 Å was indeed due to this fluorescence of OH, we used other

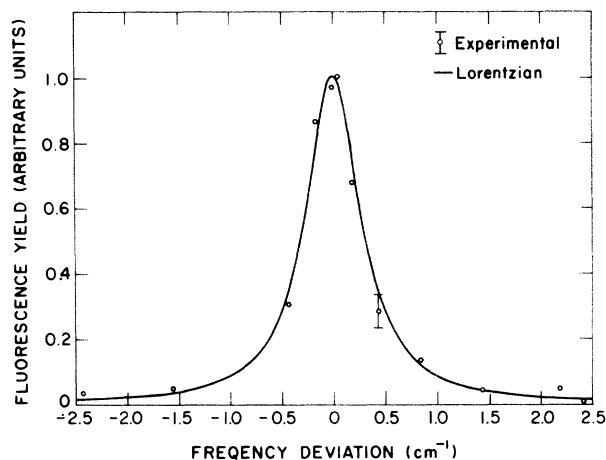


FIG. 3. Excitation spectrum in air for the $P_1(2)$ line near 2825.8 Å in the ${}^2\Pi(v=0) \rightarrow {}^2\Sigma^+(v=1)$ transitions. The experimental data were fitted by a Lorentzian with a (full width at half-maximum) intensity of 0.62 cm^{-1} , due mostly to the linewidth of the exciting radiation. The ordinate of the experimental points represents the difference between the actual measurement at a given frequency deviation and the off-resonance background count 5 cm^{-1} away from line center.

exciting frequencies corresponding to the $P_1(1)$ (2821.7 Å), $P_1(3)$ (2830.1 Å), and $R_1(2)$ (2813 Å) lines of the ${}^2\Pi(v=0) \rightarrow {}^2\Sigma^+(v=1)$ transitions of OH. It was found, as expected, that the excitation spectra for these exciting frequencies also exhibited resonance enhancement similar to that in Fig. 3, but with no detectable change in the resulting fluorescence spectrum.

The observed signal near 3090 Å could not have been due to the Raman scattering of methane and other hydrocarbons in air, as the predicted Raman signal corresponding to the actual hydrocarbon concentration in the laboratory air was too small by about 2 orders of magnitude. The possibility that the fluorescing OH radicals were generated through two-photon dissociation of water was ruled out, as the fluorescence signal (Fig. 4) depended linearly on the power of the exciting radiation. We have also established that the observed OH were not generated through dissociation of ozone in the focal region, as the fluorescence signal was independent of the ozone concentration, and disappeared altogether when *n*-butane, which reacted with OH but not with ozone, was introduced in air.

The fluorescence signal of OH excited by resonant absorption of radiation is given by

$$S = An\sigma_a\eta_F, \quad (1)$$

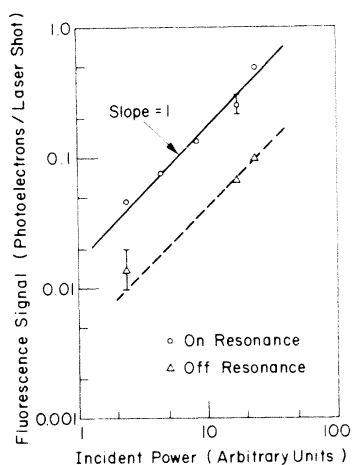


FIG. 4. Dependence of the fluorescence signal on the power of the exciting radiation. The on-resonance points were taken at the line center in Fig. 3, and the off-resonance points 5 cm^{-1} away from the line center.

where A is a measure of the excitation and detection efficiency for the particular arrangement employed in our experiments, n is the OH concentration in air, σ_a is the absorption cross section for the $P_1(2)$ transition, and η_F is the fluorescence efficiency.

For the results reported in this Letter, A was determined by comparing the OH fluorescence signal with the Raman signal of N_2 using $n(\text{N}_2) = 2.1 \times 10^{19} \text{ molecules/cm}^3$ and $\sigma_a \eta_F \rightarrow \sigma_R = 0.42 \times 10^{-28} \text{ cm}^2$ for the Raman cross section.⁷ The oscillator strength for OH transitions is well known¹; using the linewidth of the excitation spectrum in Fig. 3, one calculates that $\sigma_a = 1.2 \times 10^{-17} \text{ cm}^2$ for a room-temperature distribution. The fluorescence efficiency η_F is determined primarily by quenching of OH in the excited state through collisions with water molecules.⁸ It may be dependent both on the J' value of the excited state involved and on the total pressure of the system. One estimates that⁹ $\eta_F \approx 10^{-2}$ for our experimental conditions of 23°C and 50% relative humidity, with a probable uncertainty of a factor of 5. One then deduces from Eq. (1) that $n(\text{OH}) = 1.5 \times 10^8 \text{ radicals/cm}^3$ at the time when the data in Fig. 2 were taken. The relative uncertainties in the deduced concentrations are estimated to be about 30% at high OH concentrations and higher at lower OH concentrations (see the error bars in Figs. 3 and 4). These uncertainties are due in part to the statistical nature of the photon counting process, and in part to experimental uncertainties of our laser and detection systems. We believe

the absolute accuracy of $n\sigma_a\eta_F$ is within a factor of 3; but because of the large possible uncertainties in η_F , the deduced value for $n(\text{OH})$ may be uncertain by an order of magnitude.

In Fig. 4, the off-resonance signal was also found to change linearly with the exciting radiation. Furthermore, it varied over a wide range in the course of the day, becoming much lower as activity in the laboratory decreased. One likely source for this background signal is the fluorescence or resonant Raman scattering of ketone and other molecules which absorb at the exciting frequencies. Rough estimate indicates that resonant scattering of these pollutants in the parts-per- 10^9 range could give the background signal observed in Fig. 4. This background signal appears to be a dominating factor in determining the limit of OH detection in the atmosphere with this technique of resonance fluorescence.

The importance of detecting OH in the atmosphere was first pointed out by B. Weinstock several years ago, and the program was then formulated by R. W. Terhune. Both of them have been a constant source of encouragements and support throughout the course of the experiments. Discussion with H. Niki on the role of OH in atmospheric chemistry have been particularly enlightening.

¹R. W. Terhune, private communication; E. L. Baardsen and R. W. Terhune, *Appl. Phys. Lett.* **21**, 209 (1972).

²B. Weinstock, *Science* **166**, 224 (1969); B. Weinstock and H. Niki, *Science* **176**, 290 (1972); B. Weinstock, E. E. Daby, and H. Niki, in *Chemical Reactions in Urban Atmospheres*, edited by C. S. Tuesday (American Elsevier, New York, 1971), p. 54; H. Niki, E. E. Daby, and B. Weinstock, *Advan. Chem. Ser.* **113**, 16 (1972).

³H. Levy, II, *Science* **173**, 141 (1971); J. C. McConnell, M. B. McElroy, and S. C. Wofsy, *Science* **233**, 187 (1971).

⁴G. H. Dieke and H. M. Crosswhite, *J. Quant. Spectrosc. Radiat. Transfer* **2**, 97 (1961).

⁵L. I. Davis, Jr., and C. C. Wang, to be published.

⁶C. C. Wang, Ford Motor Company Technical Report No. SR-72-107, 1972 (unpublished); C. C. Wang and L. I. Davis, Jr., to be published.

⁷W. R. Fenner, H. A. Hyatt, J. M. Kellam, and S. P. S. Porto, *J. Opt. Soc. Amer.* **63**, 73 (1973).

⁸In Ref. 2, experiments with He and N_2 used as the carrier gas seem to indicate that quenching of the excited OH by N_2 may also be significant under atmospheric conditions. We have performed experiments at high OH concentrations (10^8 – $10^{10} \text{ radicals/cm}^3$), generated by two-photon dissociation of water (Ref. 6),

and have found that OH fluorescence is independent of water concentration and of the type of carrier gas. Since the amount of OH generated is proportional to water concentration, the observed results can be ob-

tained only if quenching is predominantly due to collisions with water molecules.

⁹D. Kley and K. H. Welge, *J. Chem. Phys.* **49**, 2870 (1968).

Linear Stability Analysis of Laser-Driven Spherical Implosions*

J. N. Shiau,† E. B. Goldman,† and C. I. Weng‡

*Laboratory for Laser Energetics, College of Engineering and Applied Sciences,
University of Rochester, Rochester, New York 14627*

(Received 1 November 1973)

A linear approximation method has been developed to study the stability of spherically symmetric hydrodynamic motion. Application of this technique to laser-driven spherical implosions indicates that the implosions are linearly unstable to perturbations at the ablating surface.

The proposed schemes^{1,3} for laser-driven implosion of deuterium-tritium pellets to the superdense state necessary for thermonuclear burning assume perfect spherical symmetry. Unavoidable departures from spherical symmetry certainly limit the compressions achievable in practice and raise the laser energy required for breakeven. Departures from symmetry during implosion arise from inherent hydrodynamic instabilities and these can be accelerated by nonuniform laser illumination. Nonuniform laser energy deposition leads to early-time nonuniform accelerations which in turn cause the earlier and more rapid growth of the instabilities.

The implosion consists of a dense layer of plasma accelerated by material being ablated into the hot, low-density blowoff (see Figs. 1 and 2). Similar conditions occur in the Rayleigh-Taylor instability which arises when two superposed fluids of different densities are accelerated in a direction perpendicular to their interface.⁴ The interface is unstable if the acceleration is directed from the less dense to the more dense fluid. For two inviscid, incompressible fluids with large density differences, separated by a plane interface, the growth rate of the perturbation on the interface is given⁴ by $\gamma = (2\pi a/\lambda)^{1/2}$, where a is the acceleration and λ the wavelength of the perturbation. For laser-driven implosions, the accelerations are $\approx 10^{16}$ cm/sec² giving growth rates of 10^9 sec⁻¹ for perturbations with wavelengths of 100 μ m. The inviscid growth rates increase for shorter wavelengths but, below a certain wavelength, dissipative effects can no longer be ignored. In addition to compressive effects, the laser-driven implosion differs from the Ray-

leigh-Taylor problem through the presence of a sharp temperature gradient and the ablating flow. These change the basic unperturbed solutions and warrant a detailed stability analysis.

The evolution of dense laser plasmas is described by a one-velocity, two-temperature set of hydrodynamic equations⁵ which include separate species temperatures and thermal conductivities as well as Coulomb energy exchange between the species. To study the stability of the flow, all of the Lagrangian variables are resolved into a zero-order, spherically symmetric component

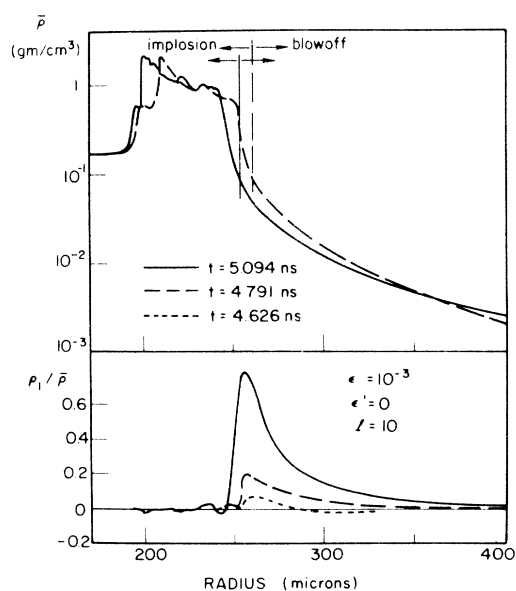


FIG. 1. Symmetric part of the density and the reduced-density perturbation versus radius at different times. Vertical lines indicate positions of ablating surface.